P-3-24

Subthreshold Current Model of Cylindrical Gate-All-Around Nanowire MOSFETs Using Analytical Solutions of Poisson's Equation

Yu-Sheng Wu and Pin Su
Department of Electronics Engineering, National Chiao Tung University, Hsinchu, Taiwan
Tel:+886-3-5712121, Fax:+886-3-5724361, E-mail: pinsu@faculty.nctu.edu.tw

Introduction

Due to its better gate control, Gate-All-Around (GAA) nanowire (NW) is an important candidate for CMOS scaling [1]-[3]. The GAA NW features the surrounding gate channel, which is an ideal structure to provide superior electrostatic behavior. Since an accurate and predictive subthreshold current model is crucial to the device and circuit design for low power applications, we provide a subthreshold current model for GAA NW using analytical solution of Poisson's equation in this paper. Using the theoretical model, the impact of channel doping and geometries on the subthreshold characteristics such as threshold voltage (V_{th}) and subthreshold swing (SS) can also be analyzed.

Potential Solution and Subthreshold Current Model

An analytical potential solution is crucial to the derivation of subthreshold current. Fig. 1 shows the schematic sketch of a GAA NW structure. The cylindrical channel is wrapped by gate insulator and connected to the gate terminal. The front and back faces are connected to the source and drain. The cylindrical GAA NW structure we consider in this study is symmetrical in θ-direction. The required boundary conditions are described in Fig. 2. This 2-D boundary value problem can be divided into two sub-problems, including 1-D Poisson's equation and 2-D Laplace equation. Using the superposition principle, the complete potential solution is $\phi = \phi_1 + \phi_2$ with ϕ_1 and ϕ_2 the solutions of the 1-D and 2-D sub-problem, respectively. The 1-D solution ϕ_1 can be expressed as

$$\phi_1(r) = -\frac{qN_a}{4\varepsilon_{si}} r^2 + V_{GS} - V_{fb} + \frac{qN_a}{\varepsilon_{si}} \frac{D}{2}\left(\frac{D}{2} + 2\frac{\varepsilon_{si}}{C_i}\right)$$

The 2-D solution ϕ_2 can be obtained using the method of separation of variables in cylindrical coordinate [5]:

$$\phi_2(r, y) = \sum_n \left[k_n \cdot \sinh(\lambda_n \cdot y) + k_n' \cdot \sinh\left(\lambda_n (L_{eff} - y)\right)\right] \cdot J_0(\lambda_n \cdot r)$$

where $J_v(x)$ is the Bessel function of the first kind of order v [5]. λ_n can be determined by

$$J_0\left(\lambda_n \frac{D}{2}\right) - \frac{\varepsilon_{si}}{C_i} \lambda_n J_1\left(\lambda_n \frac{D}{2}\right) = 0$$

The coefficients k_n and k_n' can be expressed as

$$k_n = \frac{2}{\left[(C_i/(\lambda_n \varepsilon_{si}))^2 + 1\right] \cdot J_0^2(\lambda_n D/2) \cdot \sinh(\lambda_n L_{eff})} \cdot \left\{-\left(-\frac{qN_a}{4\varepsilon_{si}}\right) \cdot \left[\frac{1}{\lambda_n}\left(\frac{D}{2}\right)^3 \cdot J_1\left(\lambda_n \frac{D}{2}\right) - 2\left(\frac{1}{\lambda_n}\right)^2 \left(\frac{D}{2}\right)^2 \cdot J_2\left(\lambda_n \frac{D}{2}\right)\right] + \left(V_{DS} - \phi_{ms} - \left(V_{GS} - V_{fb} + \frac{qN_a}{\varepsilon_{si}} \frac{D}{2}\left(\frac{D}{2} + 2\frac{\varepsilon_{si}}{C_i}\right)\right)\right) \frac{1}{\lambda_n} \frac{D}{2} \cdot J_1\left(\lambda_n \frac{D}{2}\right)\right\}$$

$$k_n' = \frac{2}{\left[(C_i/(\lambda_n \varepsilon_{si}))^2 + 1\right] \cdot J_0^2(\lambda_n D/2) \cdot \sinh(\lambda_n L_{eff})} \cdot \left\{-\left(-\frac{qN_a}{4\varepsilon_{si}}\right) \cdot \left[\frac{1}{\lambda_n}\left(\frac{D}{2}\right)^3 \cdot J_1\left(\lambda_n \frac{D}{2}\right) - 2\left(\frac{1}{\lambda_n}\right)^2 \left(\frac{D}{2}\right)^2 \cdot J_2\left(\lambda_n \frac{D}{2}\right)\right] + \left(-\phi_{ms} - \left(V_{GS} - V_{fb} + \frac{qN_a}{\varepsilon_{si}} \frac{D}{2}\left(\frac{D}{2} + 2\frac{\varepsilon_{si}}{C_i}\right)\right)\right) \frac{1}{\lambda_n} \frac{D}{2} \cdot J_1\left(\lambda_n \frac{D}{2}\right)\right\}$$

Our potential solution has been verified by 3-D ISE simulation [6]. Fig. 3 compares the derived channel potential distribution with device simulation for both lightly doped (1×10^{15}cm^{-3}) and heavily doped (3×10^{18}cm^{-3}) devices. It can be seen that our model shows satisfactory accuracy for various channel doping.

The subthreshold current can be derived using the channel potential solution. The current density $J_n(r, y)$ at the position (r, y) can be expressed as [7]:

$$J_n(r, y) = -q\mu_n n(r, y) \cdot \frac{dV(y)}{dy} = -q\mu_n \cdot \frac{n_i^2}{N_a} \exp\left[\frac{\phi(r, y) - V(y)}{kT/q}\right] \cdot \frac{dV(y)}{dy}$$

where $n(r, y)$ is the electron density at the position (r, y) and $V(y)$ is the quasi-Fermi potential. The current I_{DS} (y) can be derived by integrating in r and θ directions:

$$I_{DS}(y) = -q\mu_n \left\{-2\pi \int_0^{D/2} r \cdot \frac{n_i^2}{N_a} \exp\left[\frac{\phi(r, y) - V(y)}{kT/q}\right] dr\right\} \cdot \frac{dV(y)}{dy}$$

Since the electron current flow is continuous, the subthreshold current I_{DS} is independent of y and can obtained by

$$I_{DS} = \frac{q\mu_n (kT/q)\left(n_i^2/N_a\right)\left[1 - \exp(-V_{DS}/(kT/q))\right]}{\int_0^{L_{eff}} dy \Big/ \left[2\pi \int_0^{D/2} r \cdot \exp[q\phi(r, y)/(kT)] dr\right]}$$

Results and Discussion

Fig. 4 compares the subthreshold current of GAA NWs with 3-D ISE simulation. Fig. 4(a) shows the subthreshold current of lightly doped GAA NWs with various L_{eff}. It can be seen that with L_{eff} scaling, the SCE degrades the SS and reduces V_{th}. Fig. 4(b) shows the subthreshold current of heavily doped GAA NWs with various V_{DS}. It can be seen that with the increase of V_{DS}, drain induced barrier lowering (DIBL) reduces the V_{th} of short channel devices (L_{eff}=20nm). Our model shows satisfactory accuracy in the prediction of subthreshold current of GAA NWs.

Fig. 5 compares our GAA subthreshold current model with the experimental data from the literature [2]. The V_{th} is negative (V_{th}=−0.2V) because the device channel is undoped with n+ poly-gate. It can be seen that in the subthreshold regime, the measurement data can be bounded by the model predictions for devices with L_{eff}=30nm and L_{eff}=25nm. The comparison result validates our subthreshold current model for GAA NW.

The V_{th} and SS can be obtained by the calculated subthreshold current. We define the V_{th} as the gate voltage at which the calculated subthreshold current I_{DS}=300nA×D/L_{eff}. Fig. 6 shows the L_{eff} dependence of V_{th} for both lightly doped (1×10^{15}cm^{-3}) and heavily doped (3×10^{18}cm^{-3}) devices. It can be seen that the V_{th} of GAA NWs are sensitive to channel doping.

Fig. 7 shows that for short channel GAA NWs (L_{eff}=30nm), the SS can be improved by the scaling of channel diameter. Moreover, the SS of lightly doped devices is especially sensitive to the channel diameter. Fig. 8(a) shows that for short channel (L_{eff}=30nm) GAA NWs, the V_{th} of lightly doped devices increases with decreasing channel diameter, while the V_{th} of heavily doped ones decreases with channel diameter. For lightly doped GAA NWs, the scaling of channel diameter reduces the V_{th} roll-off and thus increases the V_{th}. However, the reverse narrow width effect (RNWE) results in the V_{th} reduction for the heavily doped devices with small diameters. Fig. 8(b) shows that the impact of RNWE on the V_{th} of heavily doped GAA NWs is more significant for long channel devices (L_{eff}=100nm).

Conclusions

We have derived a subthreshold current model for GAA

NW using analytical solutions of Poisson's equation. The accuracy of the model has been verified by TCAD simulation and experimental data. Besides, the doping and geometry dependences of the V_{th} and SS of GAA NWs have been investigated using our theoretical model. Our subthreshold current model can be used in device and circuit designs.

Acknowledgement

This work was supported in part by the National Science Council of Taiwan under contract NSC 95-2221-E-009-327-MY2, and MoE under ATU program.

References

[1] F. L. Yang *et al*., *VLSI Sym.*, p.196, 2004.
[2] S. D. Suk *et al*., *IEDM*, p.717, 2005.
[3] N. Singh *et al*., *IEEE EDL*, vol. 27, No. 5, p.383, 2006.
[4] D. K. Cheng, *Field and Wave Electromagnetics*, Addison-Wesley, 1992.
[5] D. G. Zill and M. R. Cullen, *Differential Equations with Boundary-Value Problems*, Brooks/Cole, 2001.
[6] "ISE TCAD Rel. 10.0 Manual," DESSIS, 2004.
[7] Y. Taur *et al*., *Fundamentals of Modern VLSI Devices*. Cambridge, U.K.: Cambridge Univ. Press, 1998.

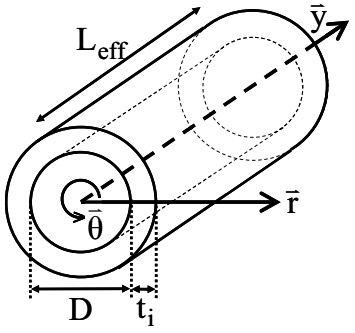

Fig. 1. Schematic sketch of the GAA structure investigated in this study. The origin point (r=0, y=0) is defined at the center of the channel/source junction.

$$\frac{\partial^2\phi(r,y)}{\partial r^2}+\frac{1}{r}\frac{\partial\phi(r,y)}{\partial r}+\frac{\partial^2\phi(r,y)}{\partial y^2}=-\frac{qN_a}{\varepsilon_{si}}$$

$$\left.\frac{\partial\phi(r,y)}{\partial r}\right|_{r=0}=0$$

$$\varepsilon_{si}\left.\frac{\partial\phi(r,y)}{\partial r}\right|_{r=D/2}=C_i\cdot\left[V_{GS}-V_{fb}-\phi\left(r=\frac{D}{2},y\right)\right]$$

$$C_i=2\varepsilon_i/\left(D\cdot\ln\left(1+2t_i/D\right)\right)$$

$$\phi(r,y=0)=-\phi_{ms}$$

$$\phi\left(r,y=L_{eff}\right)=V_{DS}-\phi_{ms}$$

Fig. 2. Boundary conditions of 2-D Poisson's equation in GAA NW structure. N_a is the channel doping. ε_{si} and ε_i are dielectric constants of Si-channel and gate insulator, respectively. Note that C_i is the capacitance per unit length for an infinite long cylindrical capacitor, which neglects the fringing effect of the field near the edges of the capacitor [4].

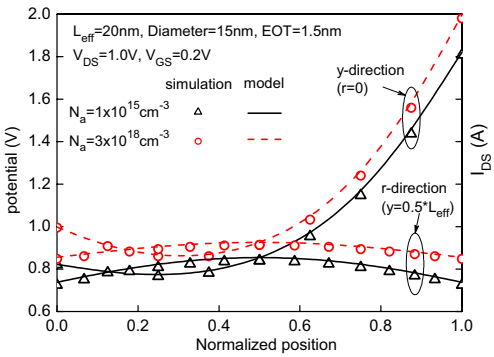

Fig. 3. Analytical potential distribution compared with the result of 3-D ISE simulation. A midgap workfunction is used (4.5eV).

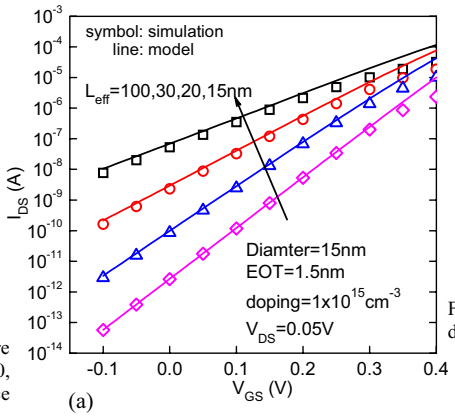

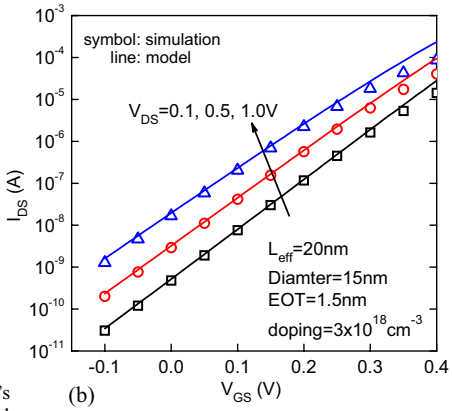

Fig. 4. Calculated subthreshold current compared with the result of 3-D ISE simulation. (a) Lightly doped channel with various L_{eff}. (b) Heavily doped channel with various V_{DS}.

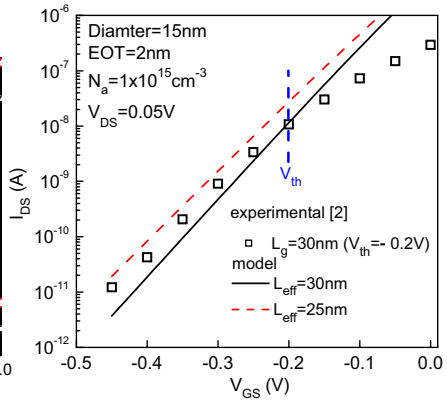

Fig. 5. Calculated subthreshold current compared with the experimental data [2]. The gate length (L_g), channel diameter and the EOT are 30nm, 15nm and 2nm, respectively.

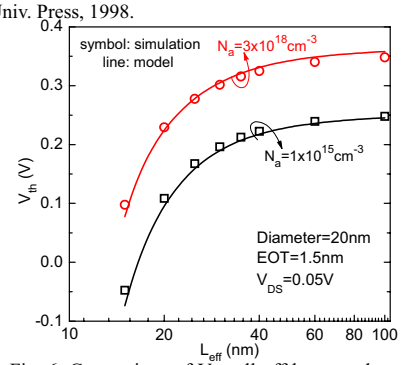

Fig. 6. Comparison of V_{th} roll-off between heavily doped and lightly doped GAA NWs.

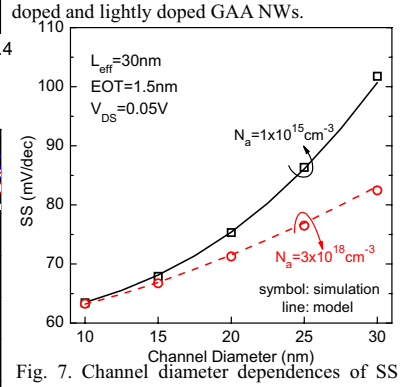

Fig. 7. Channel diameter dependences of SS for short channel GAA NWs. Both heavily doped and lightly doped devices are considered.

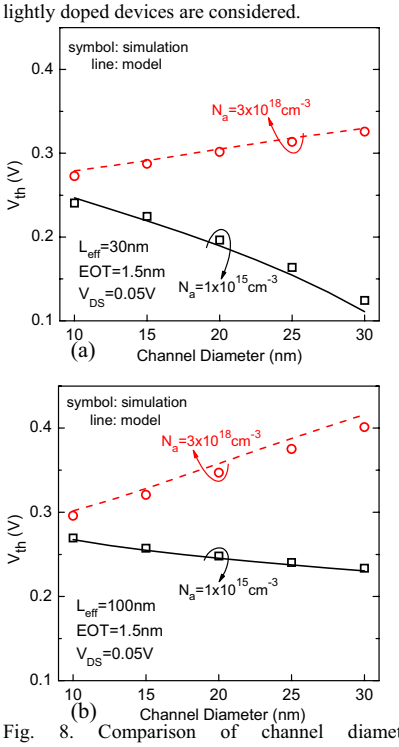

Fig. 8. Comparison of channel diameter dependences of V_{th} between heavily doped and lightly doped GAA NWs. (a) Short channel devices. (b) Long channel devices.